Int. J. Multiphase Flow, Vol. 4, pp. 383–396. Pergamon/Elsevier, 1978. Printed in Great Britain

CONFIGURATIONS OF GAS–LIQUID TWO-PHASE BUBBLES IN IMMISCIBLE LIQUID MEDIA

YASUHIKO H. MORI

Department of Mechanical Engineering, Keio University, 3-14-1 Hiyoshi, Kohoku-ku, Yokohama 223. Japan

(*Received* 15 *April* 1977)

Abstract—The configuration of a "two-phase bubble" constituted of a gas phase and a liquid phase in an immiscible liquid medium is classified into three types: complete engulfing of a gas bubble inside a liquid shell, partial coalescence of a gas bubble and a liquid drop forming a three-phase contact line, and non-coalescence whereby a gas bubble and a liquid drop remain separated. Simple criteria have been presented by which the favorable type of configuration in a given system is predicted from the values of the spreading coefficients characterizing the system. Experiments using some combinations of liquids as well as air suggest the general validity of the criteria.

INTRODUCTION

This paper deals generally with the configurations of "two-phase bubbles" constituted of a gas phase and a liquid phase in immiscible liquid media. Such two-phase bubbles appear in the following processes: rise of gas bubbles through superposed layers of two immiscible liquids (Veeraburus & Philbrook 1959; Princen & Mason 1965; Ollis, Thompson & Wolynic 1972; Li & Asher 1973; Mercier, da Cunha, Teixeira & Scofield 1974; Mori, Komotori, Higeta & Inada 1977), simultaneous injection of gas and liquid through a nozzle into an immiscible liquid (Hayakawa & Shigeta 1974), simultaneous boiling and condensation in superposed layers of two immiscible liquids (Oktay 1971; Shimada, Mori & Komotori 1977), vaporization of volatile liquid drops in an immiscible less volatile liquid (Klipstein 1963; Sideman & Taitel 1964; Prakash & Pinder 1967; Simpson, Beggs & Nazir 1973; Selecki & Gradon 1976; Tochitani, Mori & Komotori 1977), condensation of vapor bubbles in an immiscible liquid (Sideman & Hirsch 1965; Isenberg & Sideman 1970) etc. Most of these processes have been proposed for heat- or mass-transfer operations. The configurations of two-phase bubbles, in general, have some effects on the transfer rates. In some specific cases, the configurations may have crucial importance. For example, the practical utility of the novel method of blood oxygenation proposed by Li & Asher (1973) depends on whether or not the film of fluorocarbon encapsulates each oxygen bubble steadily in blood. There is no reasonable criterion available, however, for predicting the configurations.

In this paper we deduce simple criteria for the equilibrium configurations of two-phase bubbles, and then describe the experimental work performed to verify the criteria. The present study is based on a system with no rate process. It is presumed, however, that rate processes such as vaporization or condensation do not yield major influence on the configurations of two-phase bubbles unless the rates are extremely high. The experimental results by Tochitani *et al.* (1977), for example, indicate that the two-phase bubbles vaporizing in an immiscible liquid could be considered, with good approximation, to be in quasi-steady state instantaneously in the temperature-difference range of practical interest. Therefore, the results of this study will generally be applicable to the systems with rate processes as mentioned above.

PREDICTION OF CONFIGURATIONS

Possible configurations of two-phase bubbles are classified geometrically into four types as shown in figure 1. These are:

I: The gas phase is entirely enclosed by the liquid A.

II: The gas bubble and the drop of liquid *A* connect to each other so that a line bounding the three phases is formed.

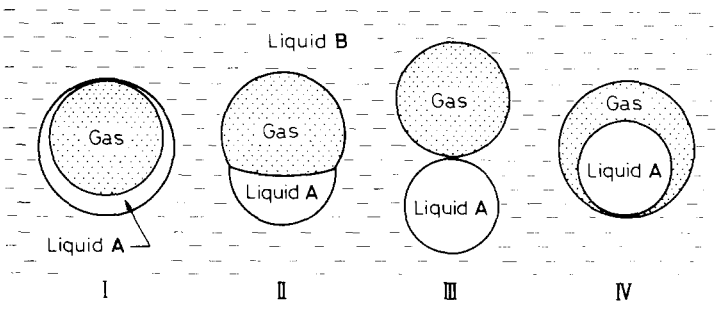

Figure 1. Possible types of configurations of two-phase bubbles.

III: The gas–liquid A interface is not present; i.e. the gas bubble and the drop of liquid A remain separated by the liquid B.

IV: The drop of liquid A is entirely enclosed by the gas phase contrary to the type I.

Here the type III is regarded as one of the types of two-phase bubbles for convenience, though it may not be in the literal sense. The total surface free energy G in each type is expressed as

$$\left.\begin{aligned}(G)_{\mathrm{I}} &= (\bar{A}_A\sigma_A + \bar{A}_{AB}\sigma_{AB})_{\mathrm{I}},\\ (G)_{\mathrm{II}} &= (\bar{A}_A\sigma_A + \bar{A}_B\sigma_B + \bar{A}_{AB}\sigma_{AB})_{\mathrm{II}},\\ (G)_{\mathrm{III}} &= (\bar{A}_B\sigma_B + \bar{A}_{AB}\sigma_{AB})_{\mathrm{III}},\\ (G)_{\mathrm{IV}} &= (\bar{A}_A\sigma_A + \bar{A}_B\sigma_B)_{\mathrm{IV}},\end{aligned}\right\} \qquad [1]$$

where $\bar{A}_A$, $\bar{A}_B$, $\bar{A}_{AB}$ denote the areas of liquid A–gas, liquid B–gas and liquid A–liquid B interfaces respectively, and σ_A, σ_B, σ_{AB} the tensions working at those interfaces. The Roman numerals outside parentheses denote the types of configurations shown in figure 1. If the effects of viscous shear at the contour of two-phase bubble and of gravity can be neglected, the equilibrium configuration will be one which has a minimum surface free energy. For the given volumes of liquid A and gas, we can estimate roughly

$$\left.\begin{aligned}(\bar{A}_A)_{\mathrm{I}} &\simeq (\bar{A}_A + \bar{A}_B)_{\mathrm{II}} \simeq (\bar{A}_B)_{\mathrm{III}},\\ (\bar{A}_{AB})_{\mathrm{I}} &\simeq (\bar{A}_{\mathrm{B}} + \bar{A}_{\mathrm{AB}})_{\mathrm{II}} \simeq (\bar{A}_B)_{\mathrm{IV}},\\ (\bar{A}_A + \bar{A}_{AB})_{\mathrm{II}} &\simeq (\bar{A}_{AB})_{\mathrm{III}} \simeq (\bar{A}_A)_{\mathrm{IV}}.\end{aligned}\right\} \qquad [2]$$

Substituting the above relations into [1] we obtain the four characteristic categories, in terms of spreading coefficients only, as the criteria for the equilibrium configurations:

$$\left\{\begin{aligned}&\mathrm{I}: && S_A>0, && S_B<0, && S_G<0,\\ &\mathrm{II}: && S_A<0, && S_B<0, && S_G<0,\\ &\mathrm{III}: && S_A<0, && S_B>0, && S_G<0,\\ &\mathrm{IV}: && S_A<0, && S_B<0, && S_G>0\end{aligned}\right\} \qquad [3]$$

where

$$\left.\begin{aligned}S_A &= \sigma_B - (\sigma_A + \sigma_{AB}),\\ S_B &= \sigma_A - (\sigma_B + \sigma_{AB}),\\ S_G &= \sigma_{AB} - (\sigma_A + \sigma_B).\end{aligned}\right\} \qquad [4]$$

Each category of the four in [3] favors one of the four types of configurations (figure 1) of the same Roman numeral. These criteria are analogous to those presented by Torza & Mason (1970) for the interactions of three immiscible liquids. Some inequalities given in [3] can be eliminated, since they are satisfied always if some other inequalities are satisfied. Furthermore, the type IV does not seem to be available, since we know no combination of liquids in which S_G takes a positive value. Therefore, the criteria of the equilibrium configurations are simplified as follows:

$$\left\{\begin{array}{ll} \text{I: } S_A > 0, & \\ \text{II: } S_A < 0, & S_B < 0, \\ \text{III: } S_B > 0. & \end{array}\right\} \qquad [5]$$

These criteria have been derived considering only surface and interfacial free energies. When two-phase bubbles rise in the gravitational field undergoing viscous shear on their surfaces, it may be necessary to modify the above criteria. The theoretical consideration given in the appendix indicates that the type I will not be available at higher values of $\mu U/S_A$ (μ: dynamic viscosity of liquid B, U: rise velocity) even though $S_A > 0$.

EXPERIMENTAL APPARATUS AND PROCEDURE

The experiments were so designed that two-phase bubbles would be formed alternatively through each process of the two; i.e. injection of an air bubble inside a drop of liquid A and injection of a drop of liquid A inside an air bubble, in a continuous phase of liquid B by use of concentric nozzles. Liquid A encloses entirely an air bubble at the initial stage irrespective of the spreading coefficients in the former process, while air encloses a drop of liquid A at the initial stage in the latter process. Figure 2 shows the construction of concentric nozzles. The tip of the outer nozzle made of Pyrex glass was covered by a Teflon film in some cases to change the wettability of the liquids. A short Teflon tube was sometimes attached to the tip of the inner nozzle made of stainless steel for the same reason.

In one process of the two, liquid A was fed through the annular space between both nozzles so that a spherical-crown-shaped drop of liquid A could be formed at the tip of the outer nozzle facing upwards. By injecting an air bubble from the inner nozzle into the drop, a two-phase bubble was released from the tip of the outer nozzle into the continuous phase because of buoyancy.

In an alternative process, liquid A and air were exchanged with each other while the nozzles were facing downwards as shown in figure 2(b). By rotating the nozzles around a horizontal axis which passes the tip of the outer nozzle, a two-phase bubble was released into the continuous phase and rose upwards.

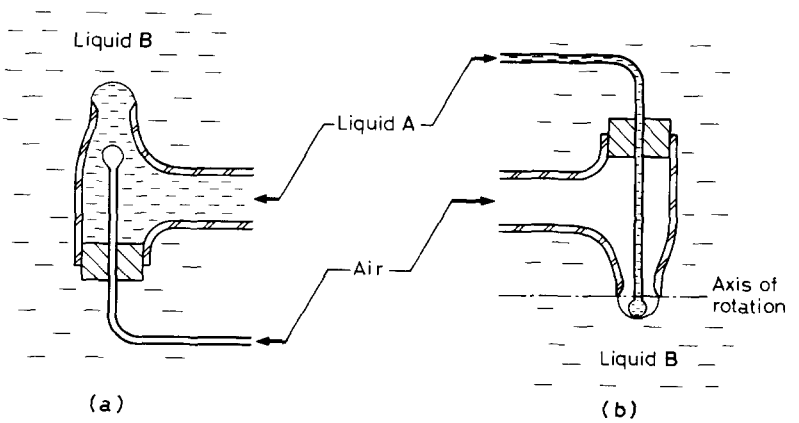

Figure 2. Construction of concentric nozzles.

The nozzles as well as test liquids were placed in a rectangular vessel made of acrylic plastics. Test liquids contacted with no material other than Pylex glass, stainless steel, Teflon and acrylic plastics.

The behaviors of formation and rise of two-phase bubbles were photographed at a rate of 9 frames per second with a 35-mm motor drive camera (Canon High-Speed Motor Drive Camera) set on a platform of slide stand. The output of the X-contact of the camera was connected to an electronic counter with a memory circuit (custom-made by Kyoei Electronic Co. Ltd., Tokyo); this made it possible to know the time lapse of succeeding frames from the first frame. The light was provided from behind the test vessel with some angle of direction to obtain a good contrast between liquids A and B. The experiments were performed in a constant temperature room, and the liquid temperatures were regulated to 20 ± 1°C.

Six systems given in table 1 were used for the experiments. The castor oil employed was industrial grade and was passed through a filter 0.45 μm pore size (Membrane Filter TM-2 made by Toyo Roshi Co. Ltd., Tokyo). Other liquids were reagent grade and no special precautions were taken to purify them further. Liquids A and B in each system were mutually saturated beforehand. The properties given in table 1 are for such combinations of liquids saturated mutually. Surface and interfacial tensions were measured with a Wilhelmy surface balance with the help of measurements of contact angles by means of the tilting-plate method.

Every system given in table 1 is represented by a point in $S_A - S_B$ plane in figure 3. The second, third, and fourth quadrants represent the characteristic categories I, II, and III given in [3] or [5]. There exists no system which falls in the first quadrant since both S_A and S_B cannot take positive values at the same time.

EXPERIMENTAL RESULTS AND DISCUSSION

Category I

R 113–86% *Aqueous glycerol.* In this system, stable two-phase bubbles were always formed by either process of the two described in the preceding section. Figure 4 shows a typical sequence of discharge of a two-phase bubble from the nozzle facing upwards. Given are the duration from the first frame, t, and the height of the top of the two-phase bubble from the tip of outer nozzle, H. These pictures do not indicate whether or not the thin film of R 113 envelops the upper part of air bubble. At the stage shown in the third frame in figure 4, for example, the non-dimensional modulus $\mu U/S_A$ is about 0.68; whereby one can deduce $\alpha =$

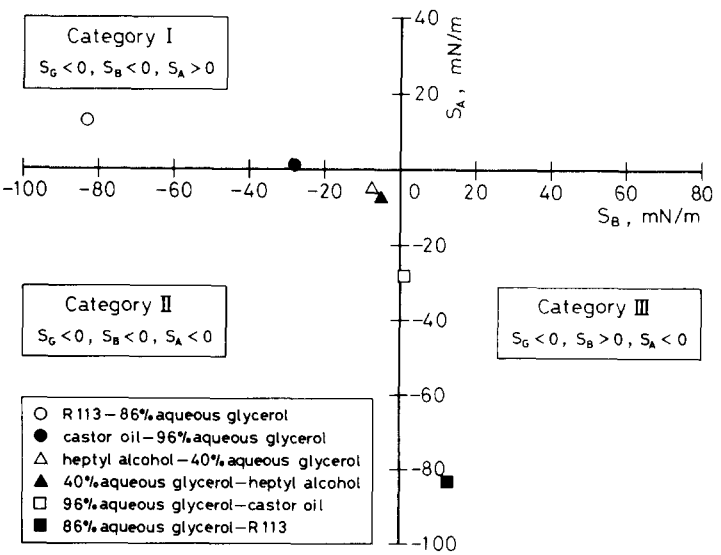

Figure 3. Spreading coefficients in the systems used.

Table 1. Properties of the systems

Liquid A–Liquid B	ρ_A (Mg/m^3)	ρ_B (Mg/m^3)	σ_A (mN/m)	σ_B (mN/m)	σ_{AB} (mN/m)	S_A (mN/m)	S_B (mN/m)	S_G (mN/m)
R 113—86% aqueous glycerol	1.575	1.226	20	68	35	13	−83	−53
Castor oil—96% aqueous glycerol	0.972	1.253	36	51	14	1	−28	−74
Heptyl alcohol—40% aqueous glycerol	0.824	1.101	27	28	6	−5	−8	−48
40% Aqueous glycerol—heptyl alcohol	1.101	0.824	28	27	6	−8	−5	−48
96% Aqueous glycerol—castor oil	1.253	0.972	51	36	14	−28	1	−74
86% Aqueous glycerol—R 113	1.226	1.575	68	20	35	−83	13	−53

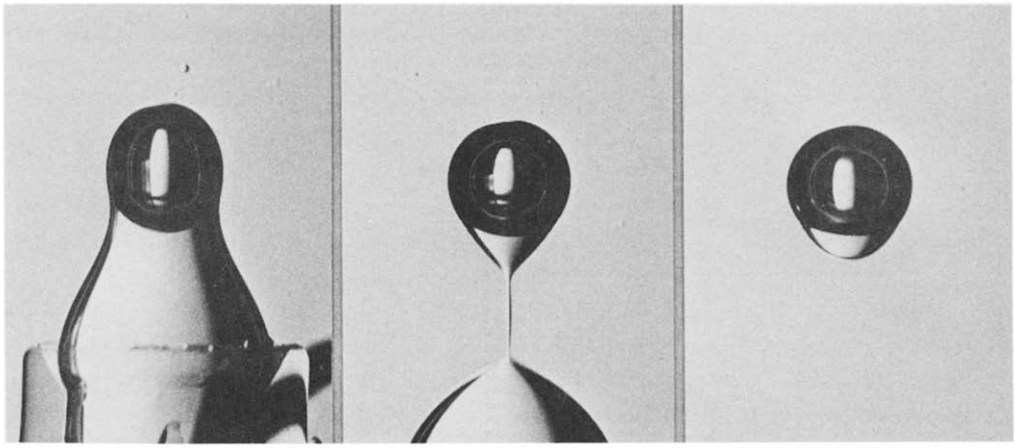

Figure 4. R 113–86% aqueous glycerol.

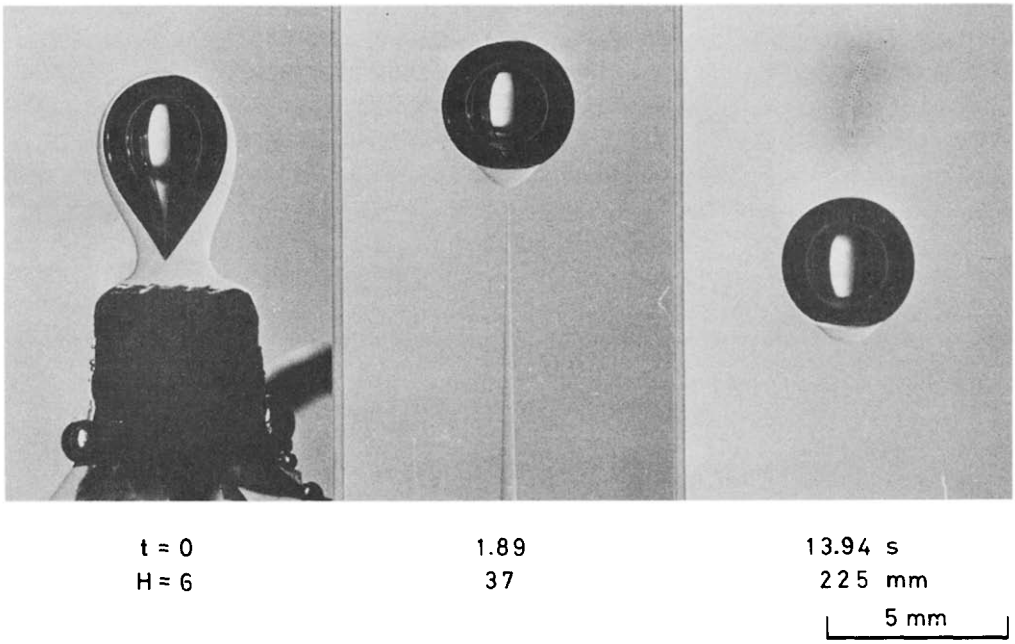

Figure 5. Castor oil—96% aqueous glycerol.

1.2 rad, assuming $\beta = 2.2$ rad based on the picture (see figures A.1 and A.2). It is likely, however, that a two-phase bubble released from the nozzle facing upwards arrives at the free surface of the aqueous glycerol about 400 mm above the nozzle tip before the film of R 113 entirely enveloping the air bubble is ruptured. No marked differences were found in the configuration of two-phase bubbles due to the difference in the process of formation.

Castor oil–96% aqueous glycerol. Stable two-phase bubbles were formed by either process. Figure 5 shows the sequence of formation of a two-phase bubble while the nozzle was facing upwards. It should be noted that the three-phase contact line is clearly perceptible on the second and third frames. This fact indicates that the rupture and the succeeding withdrawal of the film of castor oil over the bubble surface occurred at a stage before the second frame. The theory predicts that the difference of zenithal angles, $\beta - \alpha$, is about 0.14 rad at the stage shown

in the third frame, though such a film is not perceptible in the frame. This discrepancy may be ascribed partly to the small errors in measuring surface and interfacial tensions. The errors of ±1 mN/m which were inevitable in our measurements would readily cause S_A (or S_B) of small absolute value to have a wrong sign.

Category II

Heptyl alcohol–40% aqueous glycerol. The stable two-phase bubbles formed by using the nozzle facing upwards exhibited the typical configuration of type II as shown in figure 6(a) in accordance with the criteria described before. However, two-phase bubbles were not formed in an alternative process as shown in figure 6(b). A drop of heptyl-alcohol attached at the bottom surface of air bubble forming the three-phase contact line, then slid along the bubble surface because of buoyancy since ρ_A was less than ρ_B (density of liquid B), and finally detached from the bubble. Apparently the buoyancy was stronger than the force which acted at the three-phase contact line to stick the drop on to the bubble surface. An immediate blow off of air while the drop attached the bubble would result in the formation of a two-phase bubble, though we could not do such an operation successfully.

40% *Aqueous glycerol–heptyl alcohol.* Two-phase bubbles were not formed as shown in figure 7. A consideration of two spreading coefficients at the three-phase contact line indicates that the separation between an air bubble and a drop of liquid A becomes easier as S_A decreases and as S_B increases. The present system has lower S_A and higher S_B compared with the preceding system in the same category, though the differences between them are small. The density relation in the present system such as $\rho_A > \rho_B$ also promotes the detachment of the two phases as suggested by the sequence shown in figure 7(b). These factors contribute to the discrepancy between the real phenomena and the theoretical prediction.

Category III

96% *Aqueous glycerol–castor oil.* Figure 8(a) shows a sequence of formation and disruption of a two-phase bubble. A thick film of aqueous glycerol envelops the air bubble at the stage shown in the first frame, because the rate of drainage of the aqueous glycerol is very low due to its high viscosity. The film thins gradually with time as can be seen from the first to the fourth frames. The rupture of the film causes its immediate withdrawal as shown in the fifth frame, and then results in a disruption of the two-phase bubble. When the air bubble is larger, the rupture and withdrawal of the film occurs before the release from the nozzle as shown in figure 8(b).

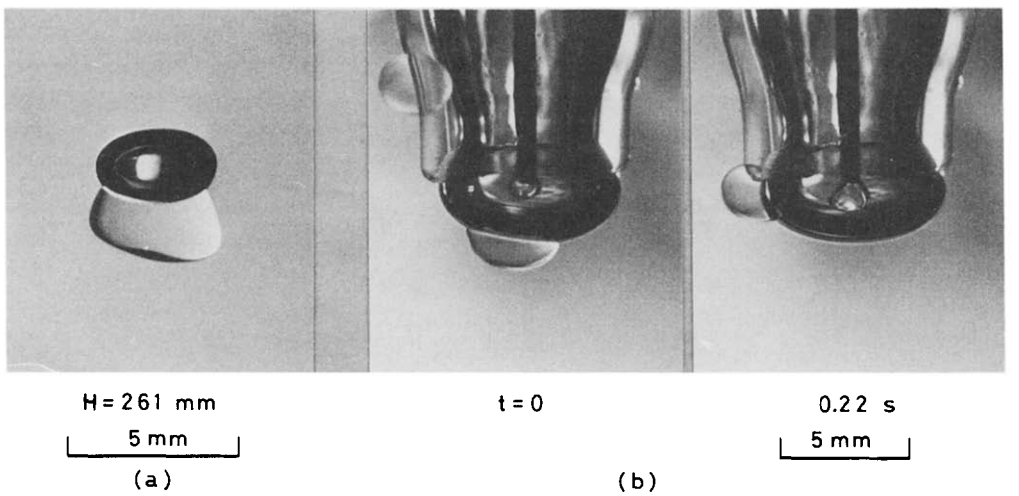

Figure 6. Heptyl alcohol—40% aqueous glycerol.

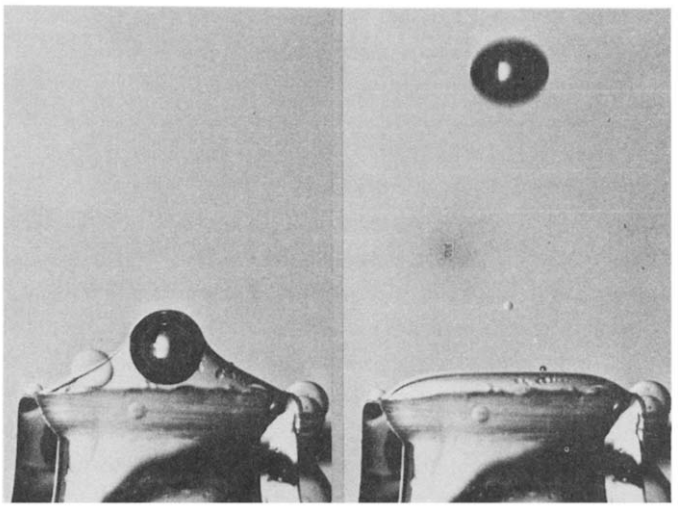

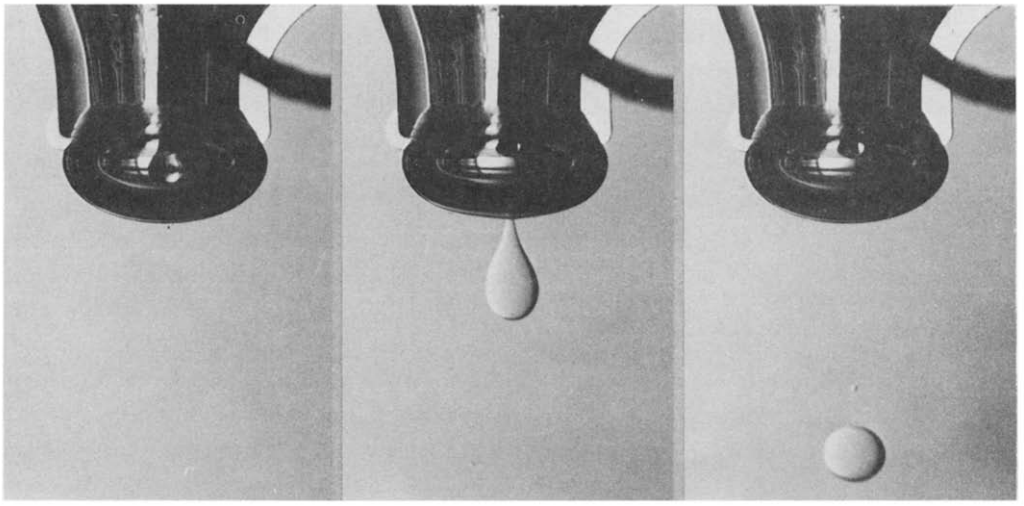

Figure 7. 40% Aqueous glycerol—heptyl alcohol.

When the nozzle faced downwards, the drops of aqueous glycerol passed through the bubble surface freely as shown in figure 8(c). Such a behavior is apparently different from that shown in figure 7(b) in which the drop of aqueous glycerol left a tail at the bubble surface.

86% *Aqueous glycerol–R* 113. The behavior shown in figure 9(a) is similar to that shown in figure 8(a) except that the disappearance of the film of liquid A and the separation between the two phases occur in a quite short time in the present system. These differences are interpreted as follows. The larger buoyancy caused by the larger density of R 113 yields the larger shear force over the film surface and then results in a rapid rupture and withdrawal of the film. Once the film disappears, the smaller S_A and larger S_B which act at the three-phase contact line favor an immediate separation between the two phases.

The relation such as $\rho_A < \rho_B$ in the present system may be unfavorable to the separation between the two phases when the nozzle facing downwards is used. As shown in figure 9(b), however, the drop of aqueous glycerol slides along the bubble surface and then detaches from the bubble. The difference between such a behavior and that shown in figure 6(b) is apparent.

SUMMARY

The configurations of two-phase bubbles can be classified geometrically into four types as shown in figure 1. A consideration of surface free energy yields the four characteristic categories I–IV, defined in terms of spreading coefficients (see [3]), each category favoring the configuration type of the same Roman numeral. The category IV is not available in the actual systems. These criteria may yield wrong predictions when the systems of interest locate near the boundaries of the categories, because of the effects of gravity and viscous shear as well as the geometrical simplifications (see [2]). The formation of two-phase bubbles has been examined experimentally using six systems extending over the three categories. The observed

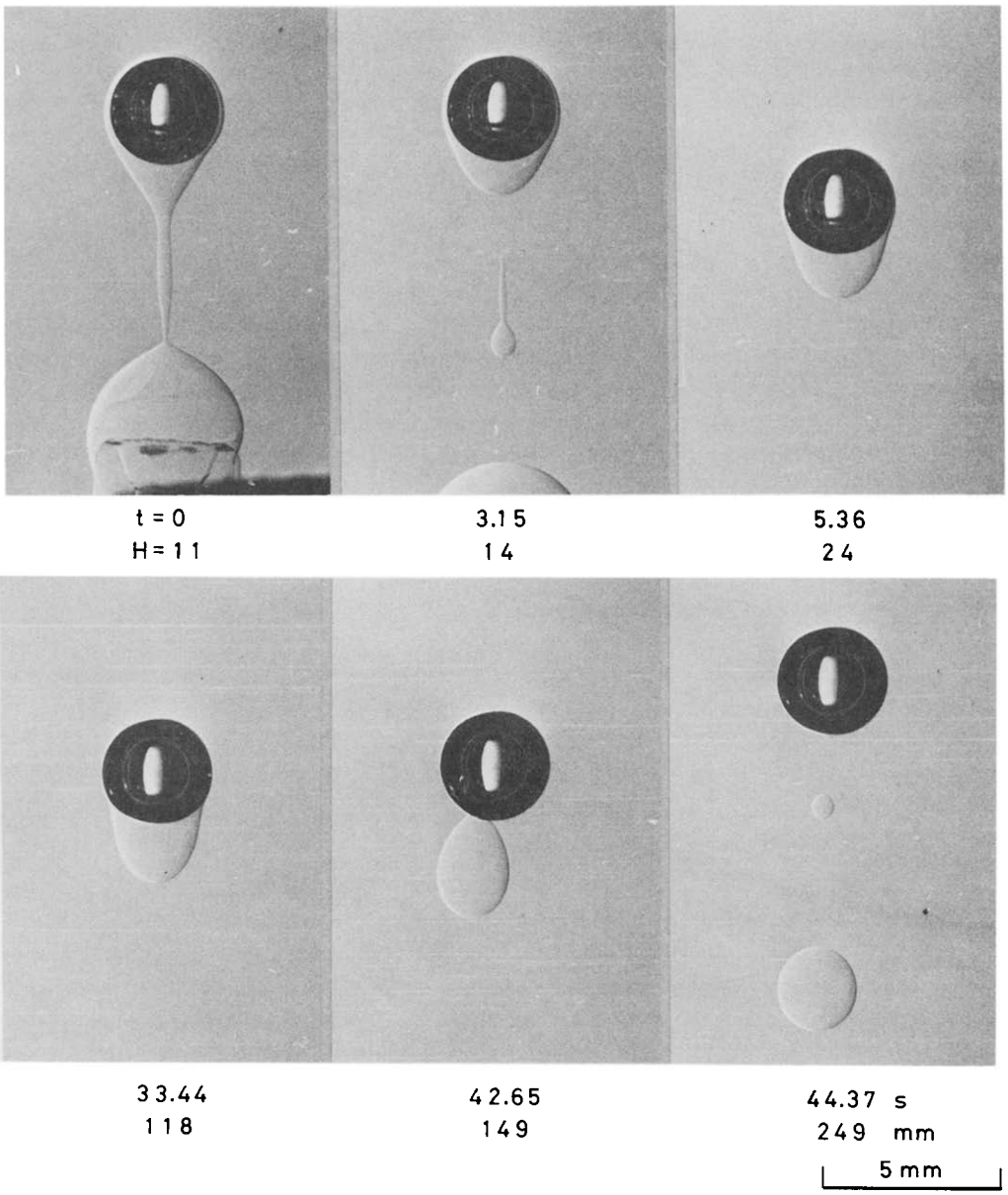

Figure 8(a).

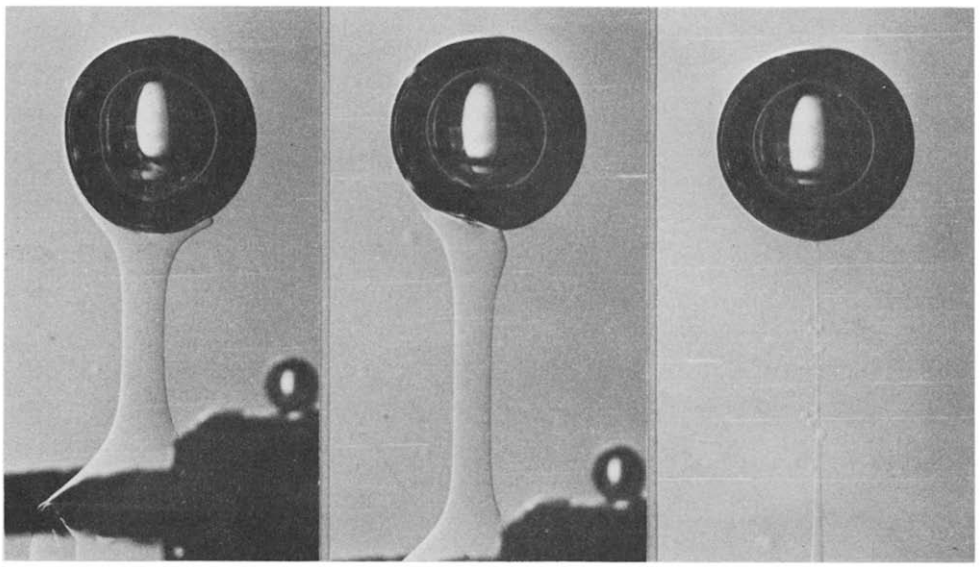

Figure 8(b).

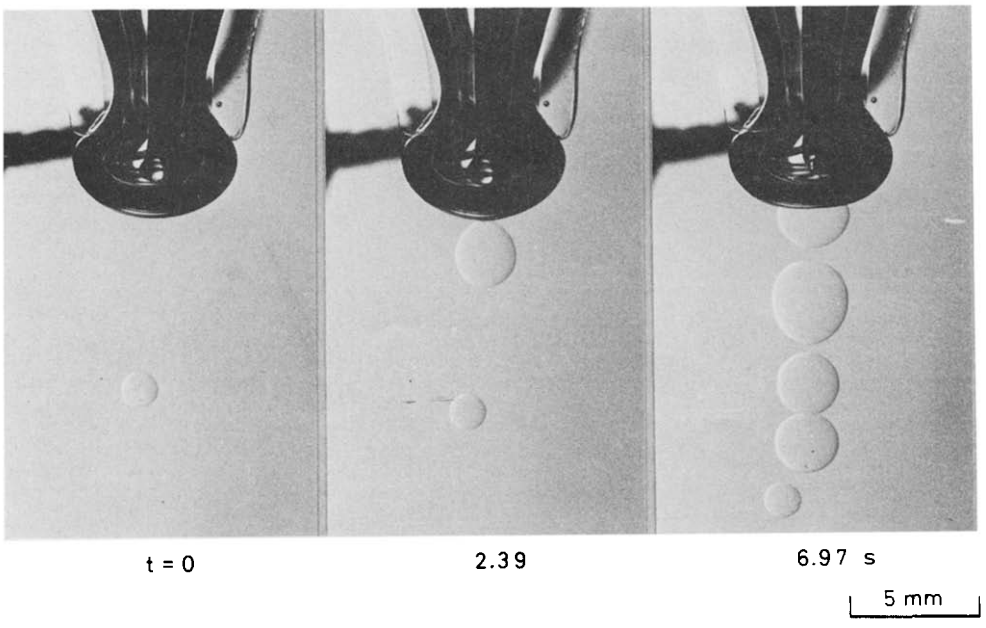

Figure 8(c).

Figure 8. 96% Aqueous glycerol—castor oil.

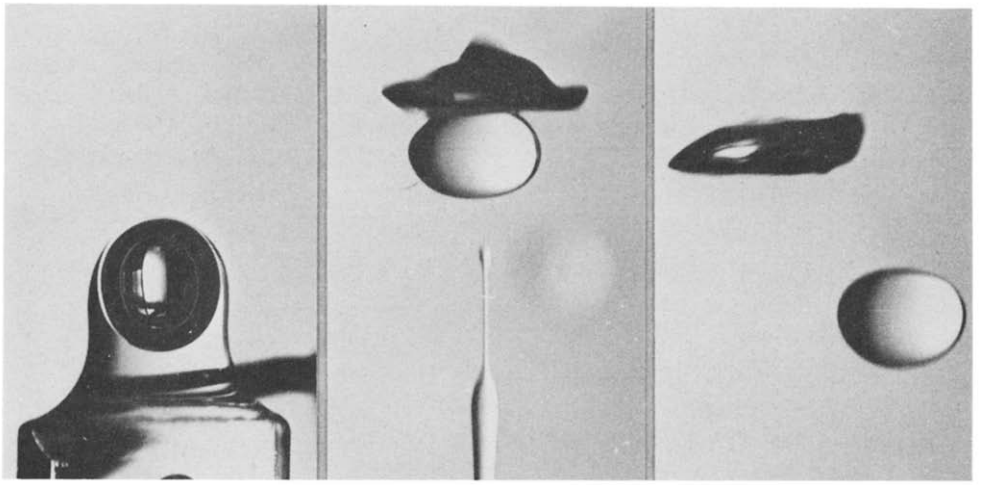

Figure 9(a).

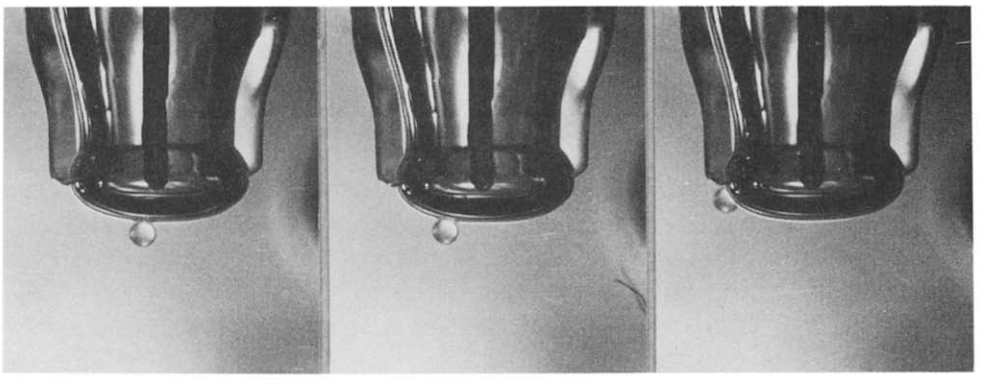

Figure 9(b).

Figure 9. 86% Aqueous glycerol—R 113.

behaviors agree generally with the above criteria, though some deviations were noted in two systems, each of them locating near the boundary of a category. These results indicate that the couple of spreading coefficients (S_A, S_B) in a given system serve as a practical index to the stability of each type of configuration in the system.

Acknowledgement—The author is indebted to Messrs. Y. Kataoka and K. Nagai for their contributions in the experiments. The present work was performed in the laboratory supervised by Prof. K. Komotori as a part of the study on "boiling heat transfer during direct contact of two immiscible liquids" subsidized by the Grant in Aid for Scientific Research of the Ministry of Education of Japan through Grant No. 155087.

REFERENCES

HAYAKAWA, T. & SHIGETA, M. 1974 Terminal velocity of two-phase droplet. *J. Chem. Engng Japan* **7**, 140–142.

ISENBERG, J. & SIDEMAN, S. 1970 Direct contact heat transfer with change of phase: Bubble condensation in immiscible liquids. *Int. J. Heat Mass Transfer* **13**, 997–1011.

KLIPSTEIN, D. H. 1963 Heat transfer to a vaporizing immiscible drop. D. Sc. Thesis, Massachusetts Inst. Technol.

LI, N. N. & ASCHER, W. J. 1973 Blood oxygenation by liquid membrane permeation. *Chemical Engineering in Medicine, Adv. Chem. Ser.* Vol. **118**, pp. 1–14. Amer. Chem. Soc.

MERCIER, J. L., DA CUNHA, F. M., TEIXEIRA, J. C. & SCOFIELD, M. P. 1974 Influence of enveloping water layer on the rise of air bubbles in Newtonian fluids. *J. Appl. Mech., Trans. Am. Soc. Mech. Engrs*, Ser. E **96**, 29–34.

MORI, Y. H., KOMOTORI, K., HIGETA, K. & INADA, J. 1977 Rising behavior of air bubbles in superposed liquid layers. *Can. J. Chem. Engng* **55**, 9–12.

OKTAY, S. 1971 Multi-fluid subdued boiling; Theoretical analysis of multi-fluid interface bubbles. *IBM J. Research Develop.* **5**, 342–354.

OLLIS, D. F., THOMPSON, J. B. & WOLYNIC, E. T. 1972 Catalytic liquid membrane reactor: I. Concept and preliminary experiments in acetaldehyde synthesis. *A.I.Ch.E.Jl* **18**, 457–458.

PRAKASH, C. B. & PINDER, K. L. 1967 Direct contact heat transfer between immiscible liquids during vaporization (Part I: Measurement of heat transfer coefficient). *Can. J. Chem. Engng* **45**, 210–214.

PRINCEN, H. M. & MASON, S. G. 1965 Shape of a fluid drop at a fluid–liquid interface (II. Theory for three-phase systems). *J. Colloid Sci.* **20**, 246–266.

SELECKI, A. & GRADON, L. 1976 Equation of motion of an expanding vapour drop in an immiscible liquid medium. *Int. J. Heat Mass Transfer* **19**, 925–929.

SHIMADA, Y., MORI, Y. H. & KOMOTORI, K. 1977 Heat transfer from a horizontal plate facing upward to superposed liquid-layers with change of phase. *J. Heat Transfer, Trans. Am. Soc. Mesh. Engrs.*, Ser. C **99**, 568–573.

SIDEMAN, S. & HIRSCH, G. 1965 Direct contact heat transfer with change of phase: Condensation of single vapor bubbles in an immiscible liquid medium. Preliminary studies. *A.I.Ch.E.Jl* **11**, 1019–1025.

SIDEMAN, S. & TAITEL, Y. 1964 Direct-contact heat transfer with change of phase: Evaporation of drops in an immiscible liquid medium. *Int. J. Heat Mass Transfer* **7**, 1273–1289.

SIMPSON, H. C., BEGGS, G. C. & NAZIR, M. 1973 Evaporation of butane drops in brine. *Proc. 4th Int. Symp. Fresh Water from the Sea* **3**, 409–420.

TOCHITANI, Y., MORI, Y. H. & KOMOTORI, K. 1977 Vaporization of single drops in an immiscible liquid (Part I, Forms and motions of vaporizing drops). *Wärme- und Stoffübertragung* **10**, 51–59.

TORZA, S. & MASON, S. G. 1970 Three-phase interactions in shear and electrical fields. *J. Colloid Int. Sci.* **33**, 67–83.

VEERABURUS, M. & PHILBROOK, W. O. 1959 Observations on liquid–liquid mass transfer with bubble stirring. *Physical Chemistry of Process Metallurgy*, Part 1; *Metallurgical society conferences* **7**, 559–578.

APPENDIX

Effect of viscous shear on the spreading of liquid A *over bubble surface*

The effect of viscous shear resulting from the translational motion is considered for a system in which S_A is positive. Such a system is favorable to the configuration type I according to the criterion given in [3] or [5].

In the gravitational field, most mass of liquid A accumulates at the bottom of the two-phase bubble (see e.g. Mori *et al.* 1977) while the residual mass may spread over the upper surface forming a thin film, depending on the value of S_A, against the gravity and viscous shear as illustrated in figure A.1. The equilibrium location of the end of the film is estimated based on the force balance over the bubble surface.

The following assumptions are introduced:

(i) The system is in steady state.

(ii) The two-phase bubble is spherical. The gas and liquid A situate in the two-phase bubble symmetrically about the vertical axis.

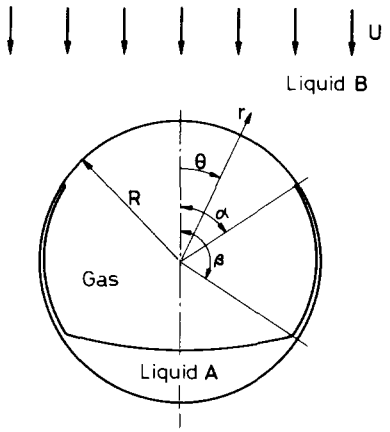

Figure A.1. Analytical model for the spreading of liquid A over bubble surface.

(iii) The two-phase bubble rises rectilinearly with a velocity U. Alternatively it can be envisioned as being at rest in the continuous medium of liquid B moving downward with an approach velocity U to it.

(iv) The film of liquid A is thin enough so that there is no circulation inside the film. From this assumption, it follows that the velocity, relative to the bubble, at $r = R$ is zero at least in the range $\alpha \leq \theta \leq \beta$, because any motion in θ direction there would change α and/or the thickness of the film, conflicting with the assumption (i).

(v) The flow around a bubble obeys Stokes' law. This assumption restricts further the consequence of the assumption (iv).

As the film thins, the overall tension of the film, σ, is no longer equal to the sum of normal tensions ($\sigma_A + \sigma_{AB}$), but varies with the film thickness. Whenever S_A is positive, σ increases with a decrease of film thickness, and thus provides the Marangoni effect along the film. For such a thin film the effect of gravity can be neglected as compared with that of viscous shear exerted on the film surface. Thus the force balance in the θ direction is described, with the aid of the assumption (v), as

$$\frac{3}{2}\frac{\mu U}{R}\sin\theta = -\frac{1}{R}\frac{d\sigma}{d\theta}, \qquad [A.1]$$

where μ denotes the dynamic viscosity of liquid B. It is reasonably presumed that the film is so formed that the surface pressure ($\sigma_B - \sigma$) vanishes at $\theta = \alpha$, because there the film meets the liquid B-gas interface with an interfacial tension σ_B. Therefore, the boundary condition at $\theta = \alpha$ is given by

$$\sigma|_{\theta=\alpha} = \sigma_B. \qquad [A.2]$$

The other boundary condition is assumed as

$$\sigma|_{\theta=\beta} = \sigma_B - S_A. \qquad [A.3]$$

This means that σ becomes equal to ($\sigma_A + \sigma_{AB}$) at the juncture $\theta = \beta$ of the film and the drop of liquid A at the bottom of bubble. Integrating [A.1] with the aid of [A.2] and [A.3], we obtain

$$\frac{\mu U}{S_A} = \frac{2}{3}\frac{1}{\cos\alpha - \cos\beta}, \qquad [A.4]$$

Figure A.2 shows the relation between α and β for various values of the parameter $\mu U/S_A$. The critical value of $\mu U/S_A$ above which the film does not envelop entirely the bubble is given by equating α to zero in [A.4] and illustrated in figure A.3.

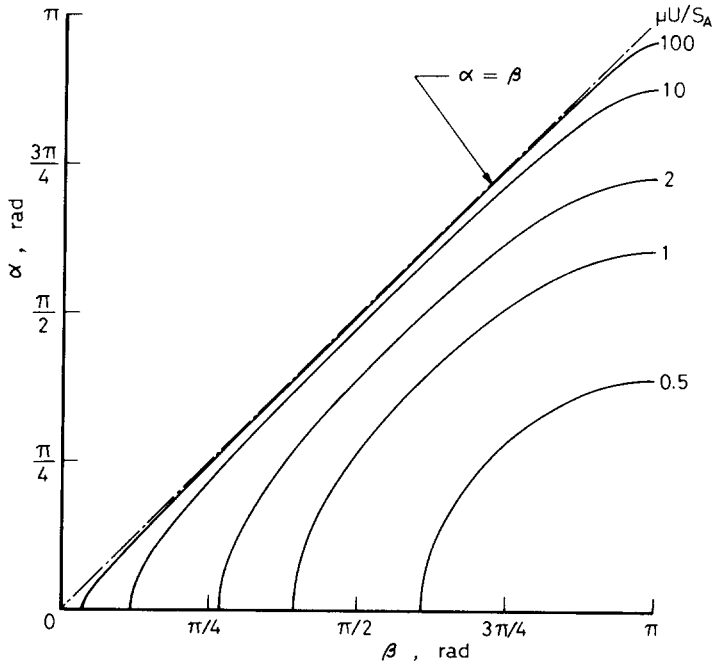

Figure A.2. Location of the end of the film of liquid A.

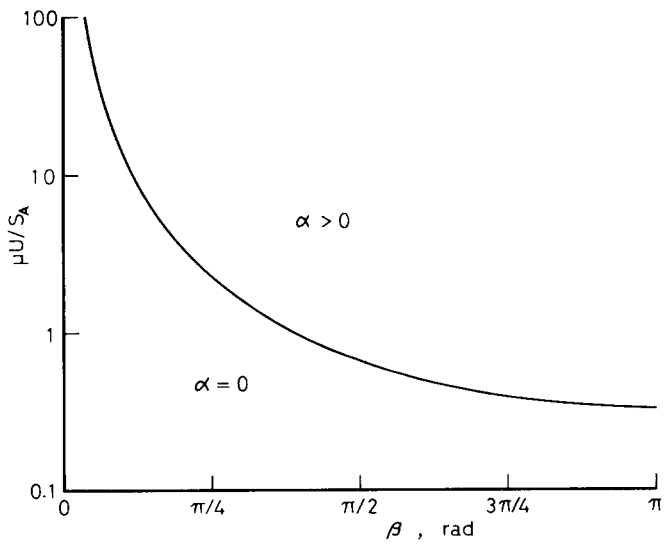

Figure A.3. Critical value of $\mu U/S_A$ for entire envelopment of bubbles by the film of liquid A.